Electronic Supplementary Material (ESI) for Journal of Materials Chemistry C.
This journal is © The Royal Society of Chemistry 2019

Hollow silica opals/cellulose acetate nanocomposite films with structural color for anti-counterfeiting of banknotes

Lin Chu, Xueting Zhang, Wenbin Niu, Suli Wu, Wei Ma, Bingtao Tang and Shufen Zhang*

State Key Laboratory of Fine Chemicals, Dalian University of Technology, Dalian 116024, P. R. China

*To whom correspondence should be addressed. E-mail: zhangshf@dlut.edu.cn

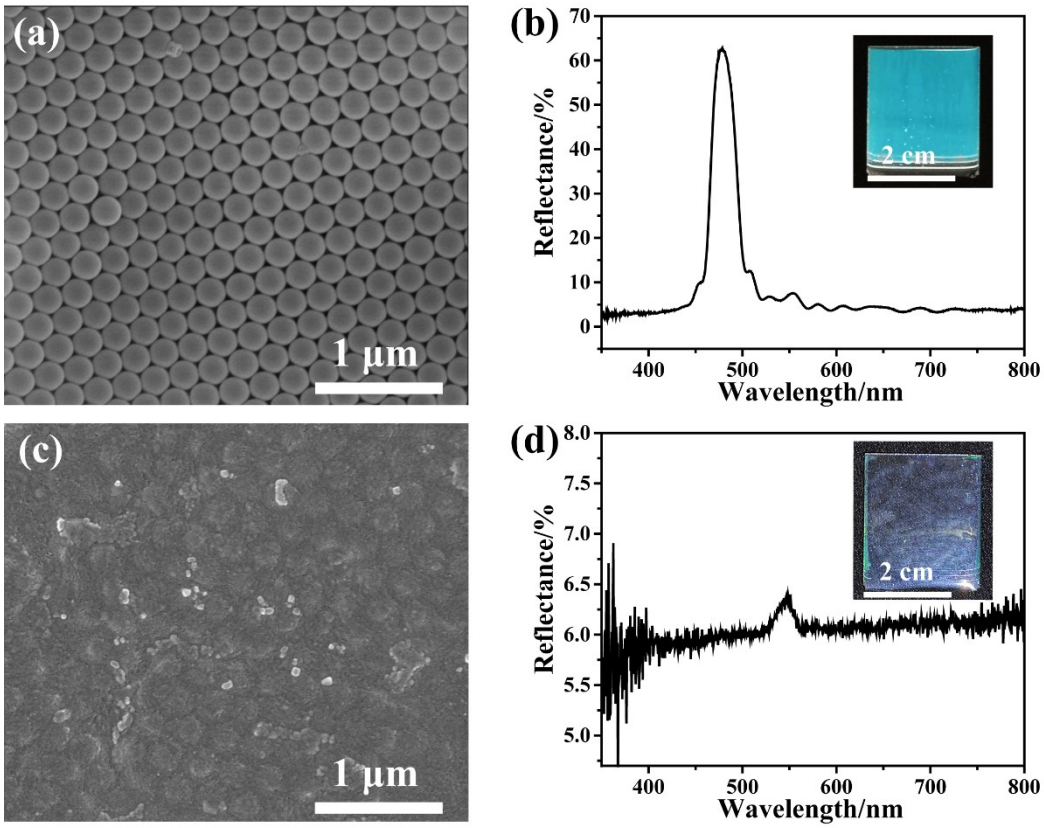

Fig. S1. Surface SEM image of SiO_2 PCs (a); (b) corresponding digital photograph and reflection spectrum of (a); (c) surface SEM image of SiO_2 PCs/cellulose acetate; (d) corresponding digital photograph and reflection spectrum of (c)

As shown in Fig. S1, solid silica PCs (Fig. S1a) were prepared by dip-coating method using the silica microspheres with the size of 221 nm. The corresponding bandgap position was at 478 nm, which exhibited brilliant blue color (Fig. S1b). After infiltrating cellulose acetate into voids of the solid silica PCs (Fig. S1c), the obtained composite film was almost transparent because of the low refractive index contrast (n silica=1.46, n cellulose=1.47). The corresponding bandgap position of composite film was at 548 nm with a weak reflectance (Fig. S1d). Hence, compared with the solid counterparts, the hollow silica (n<1.46) PCs in the composite film will offer a higher refractive index, which can enhance the brightness of structural color.

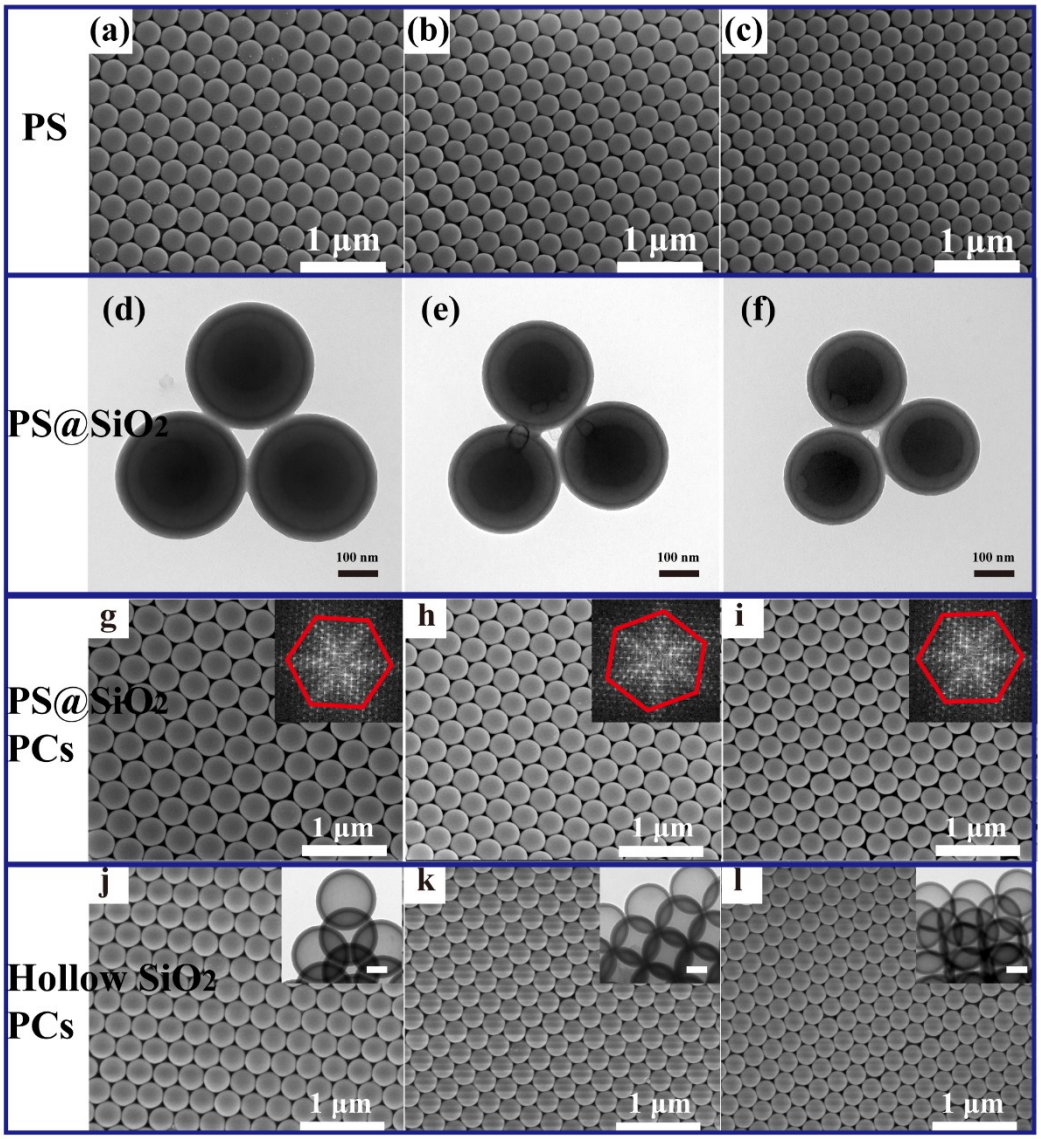

Fig. S2 SEM images of PS microspheres (a)294 nm; (b)270 nm; (c) 245 nm; (d-f) TEM images of PS@SiO_2 microspheres (d) 354 nm, (e) 314 nm, (f) 285 nm; (g-i) SEM images of PS@SiO_2 PCs (g) 354 nm, (h) 314 nm, (i) 285 nm, insets are corresponding 2D fast Fourier-transform (FFT) images; (j-l) SEM images of hollow SiO_2 PCs, (j) 296 nm, (k) 257 nm, (l) 227 nm, insets are corresponding TEM images of hollow SiO_2 microspheres.

Table S1 Diameters and Zeta-potential of three PS, PS@SiO_2 and hollow silica microspheres. Sizes were obtained via counting 200 individual particles in the SEM and TEM images of samples. PDIs are calculated by relative standard deviation. Zeta potential was measured by Dynamic Light Scattering.

Sample	Size(nm)		PDI	Zeta Potential (mV)
	diameter	shell thickness		
PS	294	/	0.016	-30.2
	270	/	0.015	-31.4
	245	/	0.017	-29.3
PS@SiO_2	354	30	0.018	-28.3
	314	22	0.017	-24.3
	285	20	0.016	-26.2
Hollow SiO_2	296	25	0.021	/
	257	19	0.024	/
	227	17	0.019	/

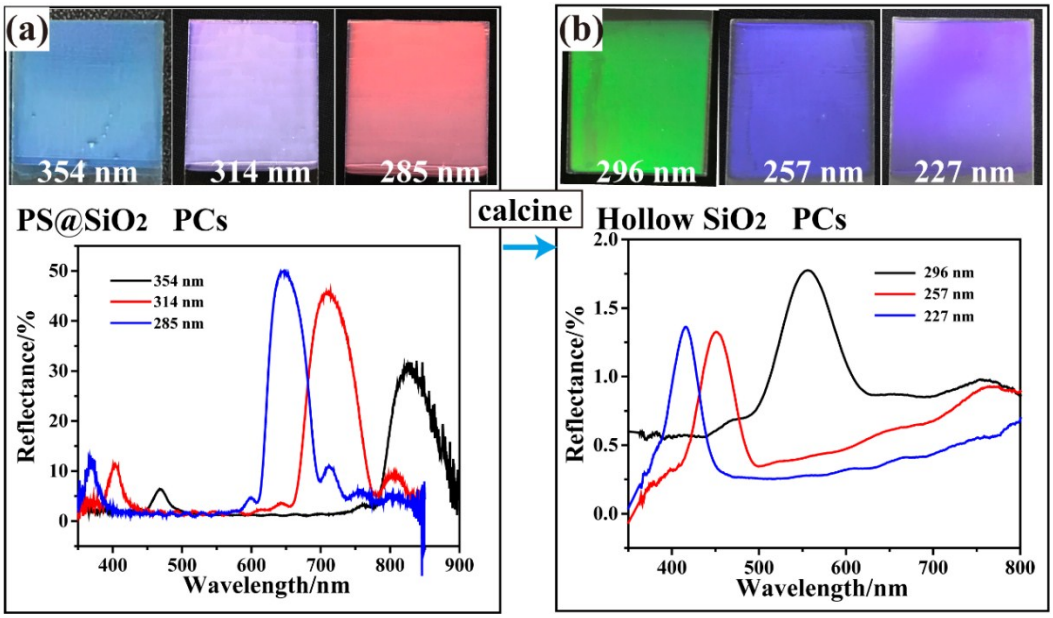

Fig. S3 The digital photographs and the corresponding reflection spectra of 3DPCs (a PS@SiO_2; b hollow SiO_2)

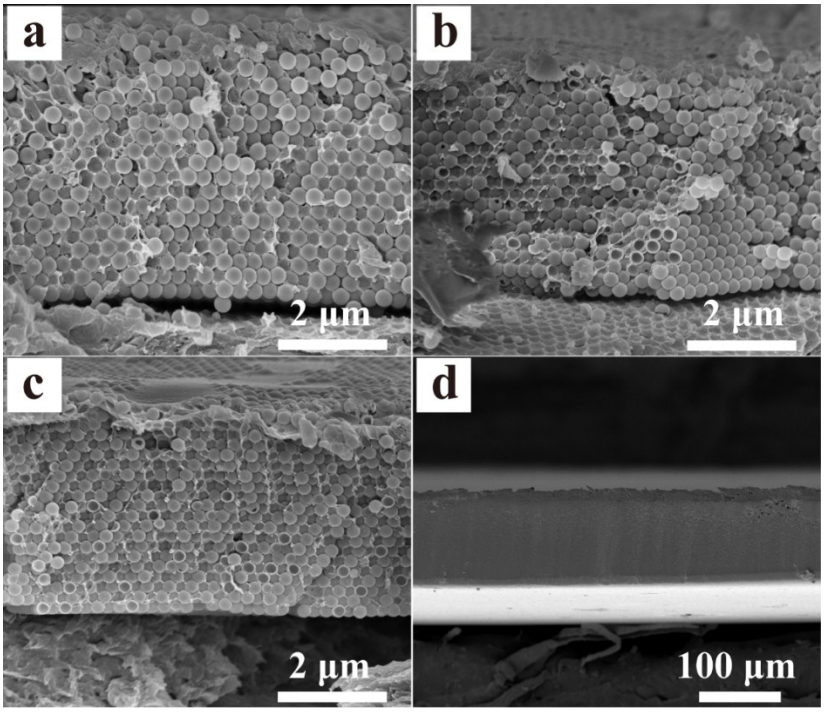

Fig. S4 The cross-sectional SEM images of hollow SiO_2/cellulose acetate nanocomposite film (a, 296 nm; b, 257 nm; c, 227 nm; d, the complete composite film)

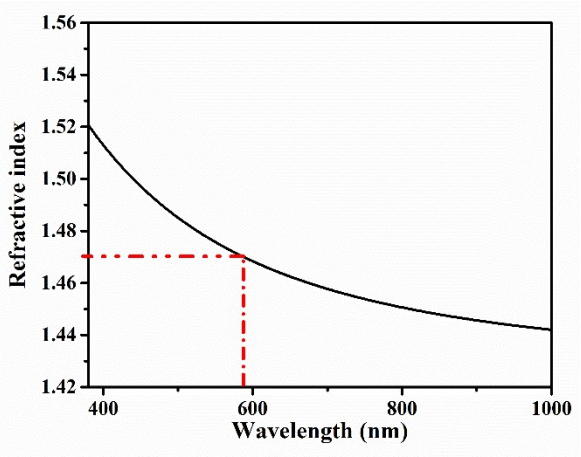

Fig. S5 Refractive index curves of cellulose acetate as a function of visible wavelength

CA film was fabricated by spin-coating method. The measurement of thickness and refractive index of CA film was performed using an M-2000 DI ellipsometer (J.A.Woollam). We defined the refractive index at the wavelength of 589 nm (1.47) as the value to be used in calculation. The thickness was 45.779 nm.

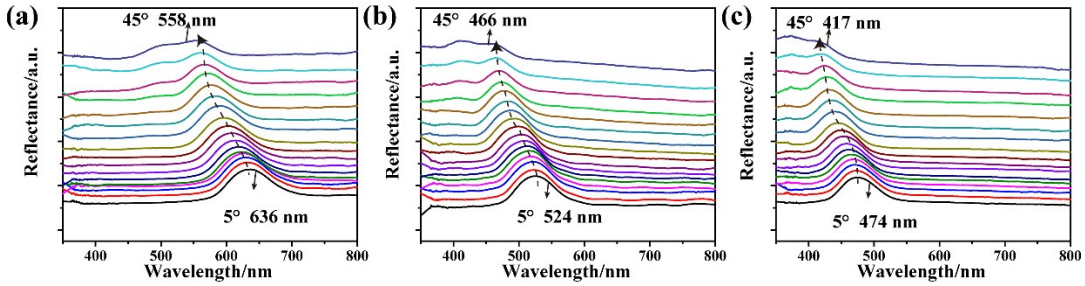

Fig. S6 Reflection spectra of hollow SiO_2/cellulose acetate films at different incident angles (a, red color; b, green color; c, blue color at incident angle from 5° to 45°)

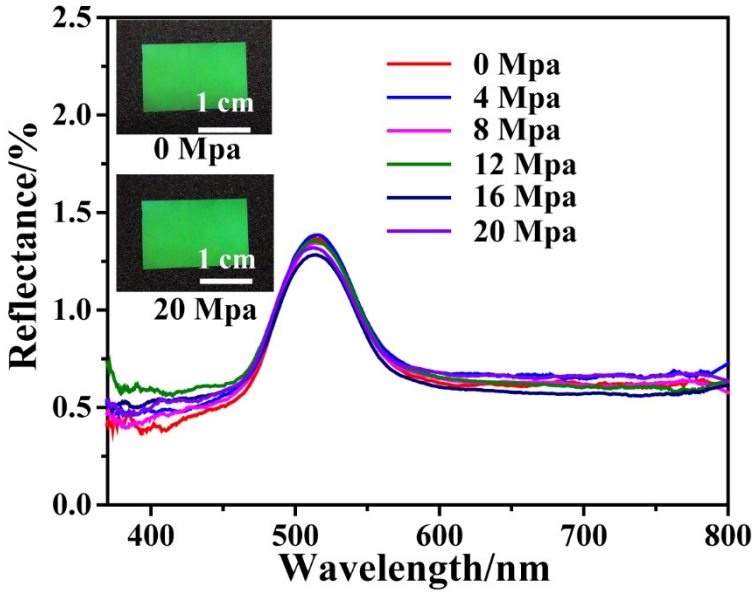

Fig. S7 Specific reflectance spectra under compression stress regularly changing from 0 to 20 MPa (257 nm hollow silica was used).

Compressive test (Fig. S7) of the composite film was conducted with a series of forces (0–20 MPa). We measured the reflection spectra under different pressure. The position of bandgap almost maintained at 520 nm, which showed that the obtained film was not fragile.

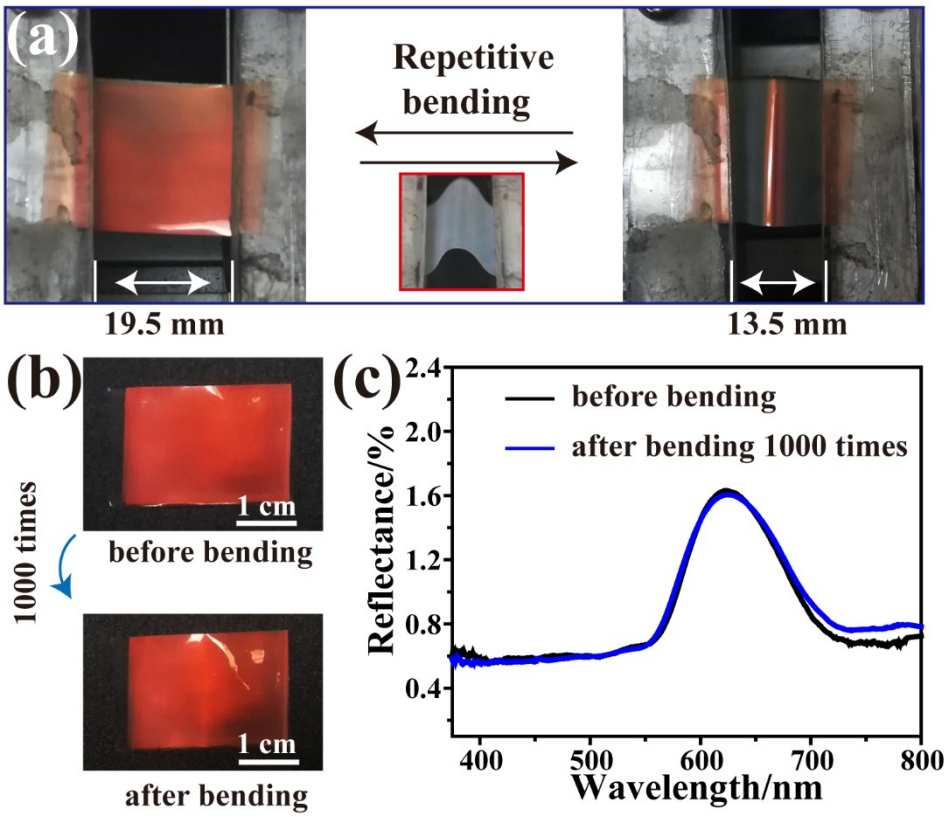

Fig. S8 (a) Equipment for the repetitive bending test; (b) digital photos of the composite film; (c) reflection spectra of the composite film before and after bending (296 nm hollow silica was used).

Repetitive bending tests were performed as shown in Fig. S8a. After bending 1000 times, the digital photo (Fig. S8b) and corresponding reflection spectra (Fig. S8c) showed that the red colored composite film maintained intact and just had some traces of bending.

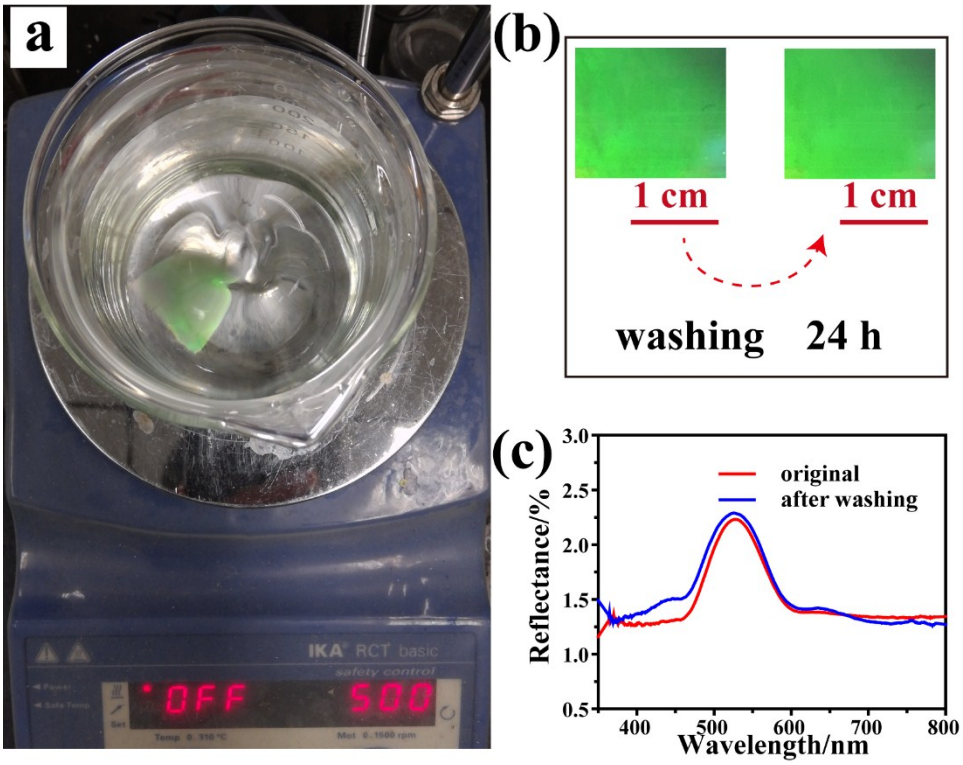

Fig. S9 (a) Equipment for the washing process; (b) digital photos of the composite film; (c) reflection spectra of the composite film before and after washing (257 nm hollow silica was used).

The simulation of washing process was shown as Fig. S9a. The green colored composite film maintained intact and did not fade after washing for 24 hours (Fig. S9b), which can be further demonstrated by the reflection spectra (Fig. S9c).

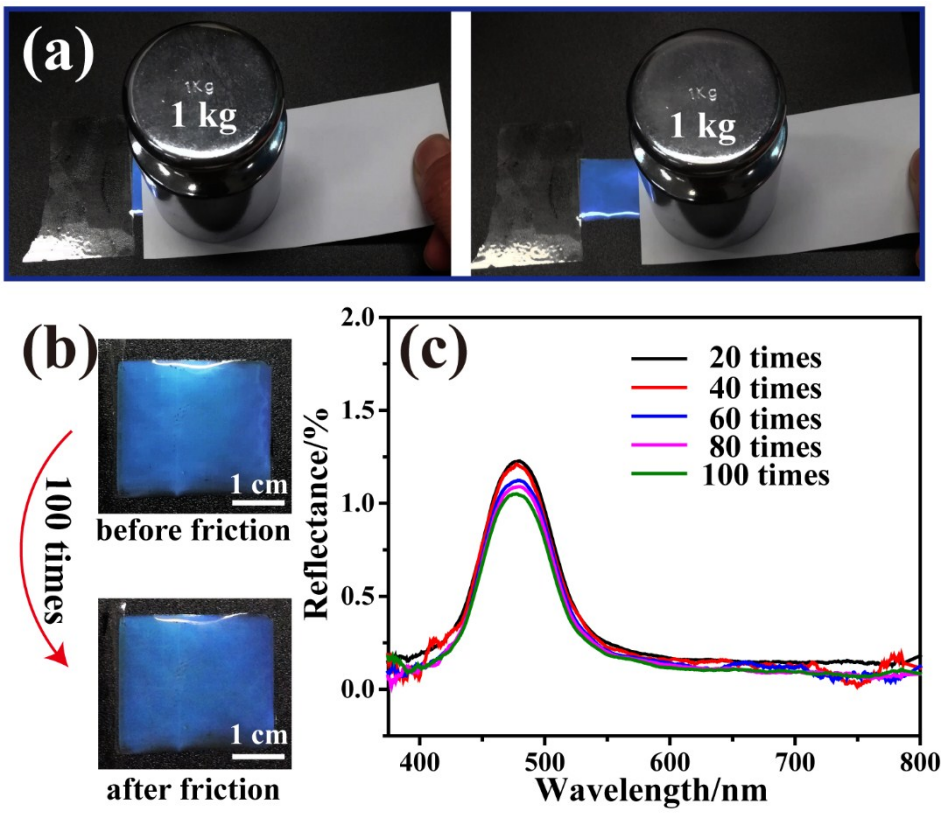

Fig. S10 (a) The digital photos of friction test; (b) digital photos of the composite film; (c) reflection spectra of the composite film before and after friction test (227 nm hollow silica was used).

The simulation of friction test was shown as Fig. S10a. A weight with 1 kg was fixed at one end of a piece of A4 paper. Then we dragged the other end of the A4 paper when the weigh was on the composite film. The process was repeated 100 times. The optical properties of the composite film remains unchanged, which can be demonstrated by the digital photos (Fig. S10b) and reflection spectra (Fig. S10c).

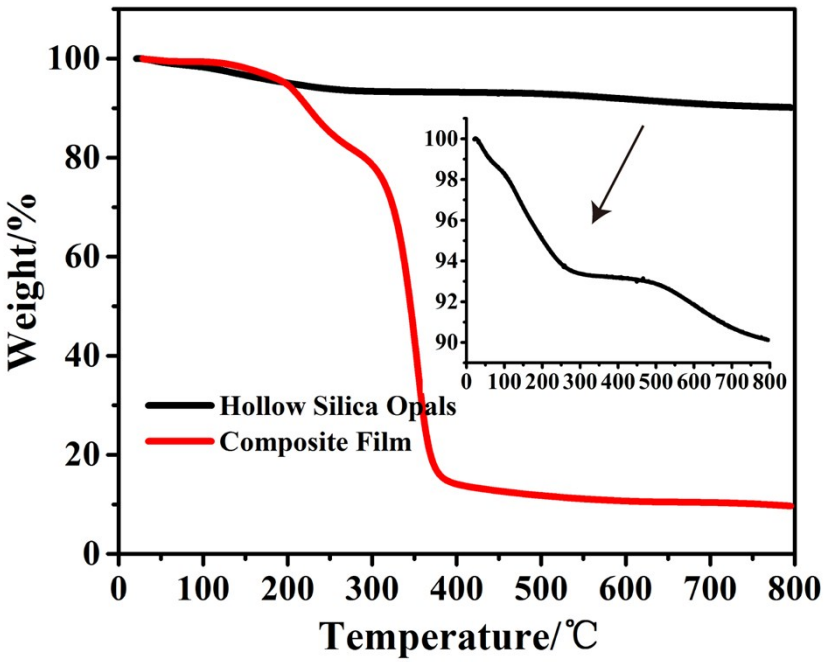

Fig. S11 TG curves of the hollow silica opals (black line) and composite film (red line) (the inset was the magnification of black line, the 227 nm hollow silica was used).

Thermal stability of hollow silica opals and the composite film was characterized using TGA. As shown in Fig. S11, when the temperature reached at 800 °C, the weight losses hollow silica opals was just about 10% because of the dehydration from condensation reaction between the silicon hydroxyl. Except for the weak weight losses of the hollow silica, the composite film underwent a two-step degradation process. The first step occurred around 250 °C because of the evaporation of plasticizer diethyl phthalate (boiling point, 296 °C) under atmosphere of N_2. The second step occurred at 300 °C because of the decomposition of cellulose acetate. Based on these results, we can easily deduce that thermal stability of the composite film is good enough for anti-counterfeiting application of banknotes.

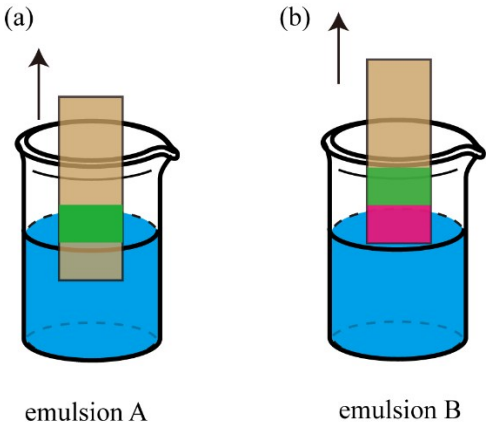

Fig. S12 Schematic diagram of the regional dip-coating method
A PS@SiO2 photonic crystal template with two diameters was prepared by regional dip-coating method. Firstly, a piece of glass slide was immersed in emulsions A, and dip coated a certain height (Fig. S12a). And we clean the part which was immersed in emulsion A, then the glass was put in emulsion B for dip-coating process (Fig. S12b).

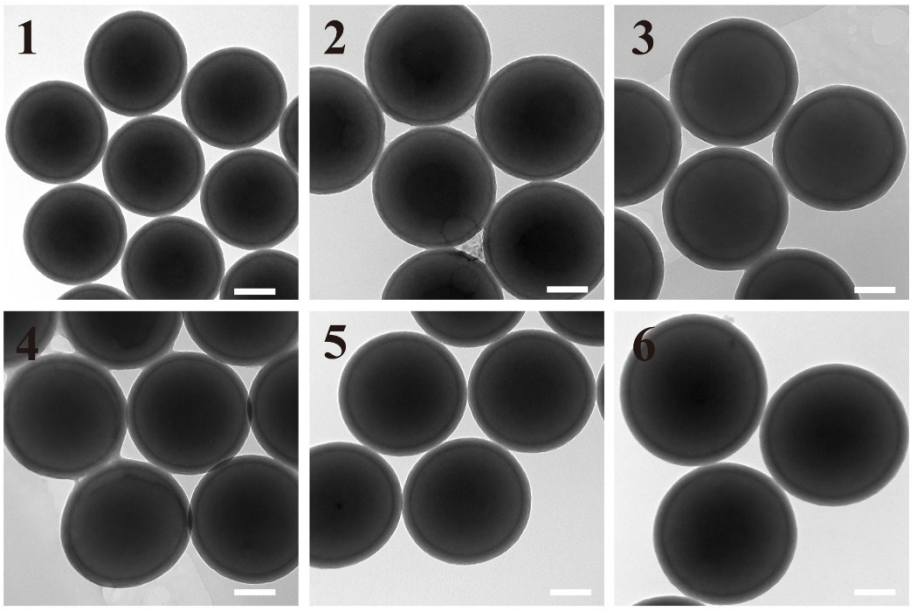

Fig. S13 TEM images of PS@SiO_2 microspheres using for fabrication of double colored composite film (1-6 corresponding to 1-6 in Figure 4e, scale bar, 1 μm, 1-6 diameters of core: 245, 294, 270, 300, 300, 324 nm, thicknesses of shell: 26, 27, 33, 23, 25, 29 nm)

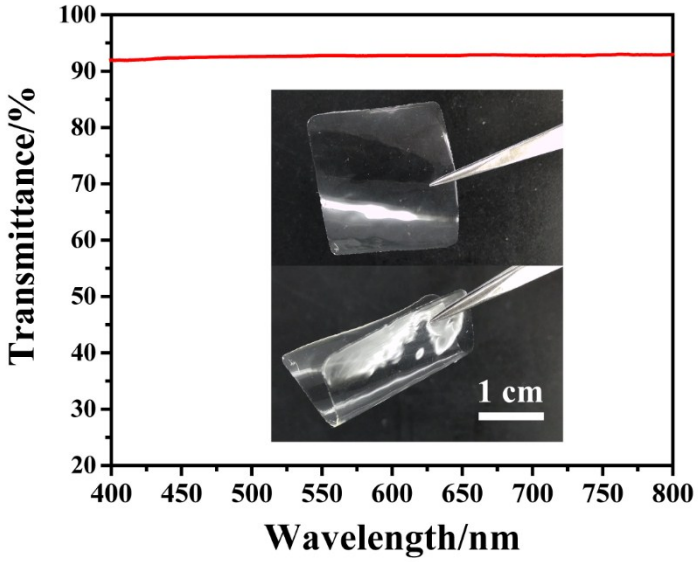

Fig. S14 The transmission spectra of bare CA film (insets are the photograph of CA film)

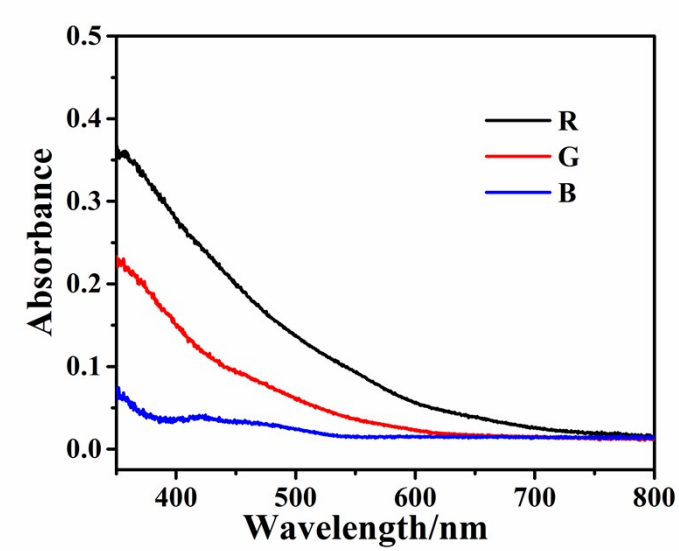

Fig. S15 Absorption spectra of the three hollow silica/cellulose acetate composite films corresponding to Fig. 5a-c

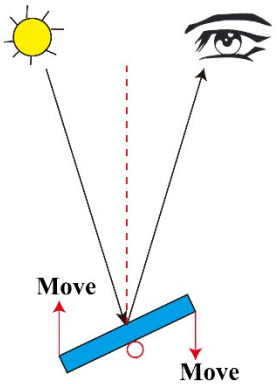

Fig. S16 Schematic diagram for recording video